

RESEARCH

Open Access



# Depletion of NUA2 blocks the stemness and angiogenesis and facilitates senescence of lung adenocarcinoma cells via enhancing ferroptosis

Jun Fan<sup>1</sup>, Lei Xue<sup>1</sup>, Haoran Lin<sup>1</sup> and Jinhua Luo<sup>1\*</sup>

## Abstract

**Background** NUA2 family kinase 2 (NUAK2) has been identified as an important mediator for tumor progression in multiple malignancies. Nevertheless, its role in lung adenocarcinoma (LUAD) remains unclear.

**Methods** Bioinformatic analysis was performed to assess the expression and prognosis of NUA2 in patients with LUAD. The NUA2 expression was measured in multiple LUAD cell lines, and the loss-of-function experiment was conducted. Cell proliferation ability was assessed using CCK-8 and colony formation assays. Spheroid formation, alkaline phosphatase (AP) staining, tube formation and SA- $\beta$ -gal staining assays were performed to examine stemness, angiogenesis and senescence. Lipid peroxidase was assessed by TBARS production and lipid ROS. Western blot was used to detect critical proteins. In addition, A549 cells were treated with ferroptosis inhibitor ferrostatin-1 (Fer-1) for a rescue assay. Finally, A549 cells were subcutaneously injected into the right flank of mice to establish LUAD-bearing mouse model, and the tumor weight and size were detected.

**Results** NUA2 was upregulated in patients with LUAD and LUAD cell lines. NUA2 depletion inhibited cell viability, colonies, tumor spheres and decreased Oct4 and Nanog expression, confirming NUA2 depletion inhibited proliferation and stemness of A549 cells. Meanwhile, NUA2 depletion blocked angiogenesis via reducing formed tubes and VEGFR1/2 expression, and promoted senescence of A549 cells by elevating SA- $\beta$ -gal-positive cells and p16, p21 and p53 expression. Moreover, NUA2 depletion elevated lipid ROS, TBARS production and Fe<sup>2+</sup> level, demonstrating that NUA2 depletion could trigger ferroptosis in A549 cells. Furthermore, the rescue experiments revealed that the impacts of NUA2 depletion on malignant behaviors in A549 cells were partly weakened by additional Fer-1 treatment. Finally, in vivo experiments demonstrated that NUA2 knockdown greatly inhibited tumor growth in LUAD-bearing mice.

**Conclusion** In summary, NUA2 depletion impeded oncogenic phenotypes of A549 cells partly via triggering ferroptosis, suggesting NUA2 as a novel target for treating LUAD.

<sup>†</sup>Jun Fan and Lei Xue contributed equally.

\*Correspondence:  
Jinhua Luo  
luojhgolden@163.com

Full list of author information is available at the end of the article



© The Author(s) 2024. **Open Access** This article is licensed under a Creative Commons Attribution-NonCommercial-NoDerivatives 4.0 International License, which permits any non-commercial use, sharing, distribution and reproduction in any medium or format, as long as you give appropriate credit to the original author(s) and the source, provide a link to the Creative Commons licence, and indicate if you modified the licensed material. You do not have permission under this licence to share adapted material derived from this article or parts of it. The images or other third party material in this article are included in the article's Creative Commons licence, unless indicated otherwise in a credit line to the material. If material is not included in the article's Creative Commons licence and your intended use is not permitted by statutory regulation or exceeds the permitted use, you will need to obtain permission directly from the copyright holder. To view a copy of this licence, visit <http://creativecommons.org/licenses/by-nc-nd/4.0/>.

**Keywords** Lung adenocarcinoma, NUAK2, Ferroptosis, Stemness, Senescence

## Introduction

Lung cancer ranks among the highest-incidence malignant solid tumors and has become the leading cause of cancer-related deaths globally, among which non-small cell lung cancer (NSCLC) is the main pathological type accounting for 85% of all lung cancer cases and exhibits a significant growth trend annually [1]. Histologically, NSCLC can be further classified into lung adenocarcinoma (LUAD), lung squamous cell carcinoma, and large cell lung cancer. LUAD is the most prevalent histological subtype of lung cancer accounting for beyond 40% of NSCLC [2]. Despite great improvements at multimodal therapy such as chemotherapy, molecular targeted therapy and immunotherapy over the past several decades, prognosis of patients with lung cancer is still not satisfactory [3]. Herin, it is critical to identify novel therapeutic strategies for LUAD treatment.

Accumulating documents reveal that ferroptosis, a dynamic tumor suppressor, is deeply implicated in cancer initiation and progression [4]. Ferroptosis is a new type of regulated cell death and is characterized by excessive accumulation of lipid peroxides and reactive oxygen species (ROS) via an iron-dependent mechanism [5]. Previous reports reveal that ferroptosis is silenced in lung cancer while activated ferroptosis can restrict lung cancer cell proliferation, migration and invasion, thereby retarding tumor development [6, 7]. Thus, ferroptosis may be a promising target for developing effective therapeutic strategies for LUAD treatment.

NUAK family kinase 2 (NUAK2), located on chromosome 1q32.1, is a member of the AMP-activated protein kinase family and has been recognized as an essential activator for YAP-driven overgrowth, stem cell expansion and tumorigenesis [8, 9]. Recently, a number of studies have confirmed that the deregulation of NUA2 contributes to the tumorigenesis and metastasis of various malignant tumors. For instance, NUA2 is upregulated in gastric cancer tissues, and NUA2 overexpression is demonstrated to promote gastric cancer cell proliferation [10]. Meanwhile, OTUD7B can accelerate gastric cancer procession through upregulating NUA2 expression [11]. Further, the upregulated NUA2 is also found in breast cancer, and NUA2 upregulation can promote tumorigenesis of breast cancer while knockdown of NUA2 retards the tumorigenesis of breast cancer [12, 13]. Nevertheless, up to date, whether NUA2 is dysregulated in LUAD remains unknown. It is interesting to find that NUA2 has been proved to inhibit glutathione peroxidase 4 (GPX4) and promote ferroptosis in breast cancer, suggesting that NUA2 may act as a ferroptosis activator [14]. Taken the critical role of ferroptosis during

LUAD development into consideration, whether NUA2 participates into the pathological processes of LUAD development through regulating ferroptosis is deserved to be explored.

Therefore, this study is designed to investigate the regulatory role of NUA2 in LUAD, and also attempt to clarify its molecular mechanism associated with ferroptosis. Our study identifies NUA2 as a novel promising target for developing potential therapies in LUAD.

## Results

### NUAK2 is upregulated in LUAD

First, ENCORI database was adopted to obtain the information of NUA2 expression in LUAD. As exhibited in Fig. 1A that compared to the normal samples, the expression level of NUA2 was elevated in tumor samples. Meanwhile, as predicted from Kaplan-Meier Plotter, patients with higher NUA2 predict lower probability of the survival time (Fig. 1B), suggesting NUA2 as a tumor promoter. Next, the expression level of NUA2 was validated again in a series of LUAD cell lines. As exhibited in Fig. 1 C-D that compared to the BEAS-2B cells, both mRNA level and protein expression of NUA2 were significantly increased in LUAD cell lines, including HCC827, PC-9, A549 and NCI-H1975 cells. Of note, A549 cells presented highest NUA2 expression among all cell lines, and thus A549 cells were used in the further experiments.

### NUAK2 depletion blocks the proliferation and stemness of A549 cells

To explore the regulatory role of NUA2 in LUAD, A549 cells were transfected with sh-NUAK2-1 or sh-NUAK2-2 to achieve knockdown of NUA2. Attributed to a superior transfection efficacy, sh-NUAK2-2 was selected in following experiments (Fig. 2A-B). Subsequently, CCK-8 assay and colony formation assay revealed that NUA2 knockdown significantly inhibited cell viability and reduced colonies (Fig. 2 C-D), demonstrating the anti-proliferative ability of NUA2 knockdown in A549 cells. In addition, according to sphere formation and alkaline phosphatase (AP) staining assays, reduced tumor spheres in sh-NUAK2 group were observed, in comparison to sh-NC group (Fig. 2E). Meanwhile, the protein expression of Oct4 and Nanog was greatly declined following NUA2 knockdown (Fig. 2F), revealing that NUA2 knockdown could restrict the stemness of A549 cells.

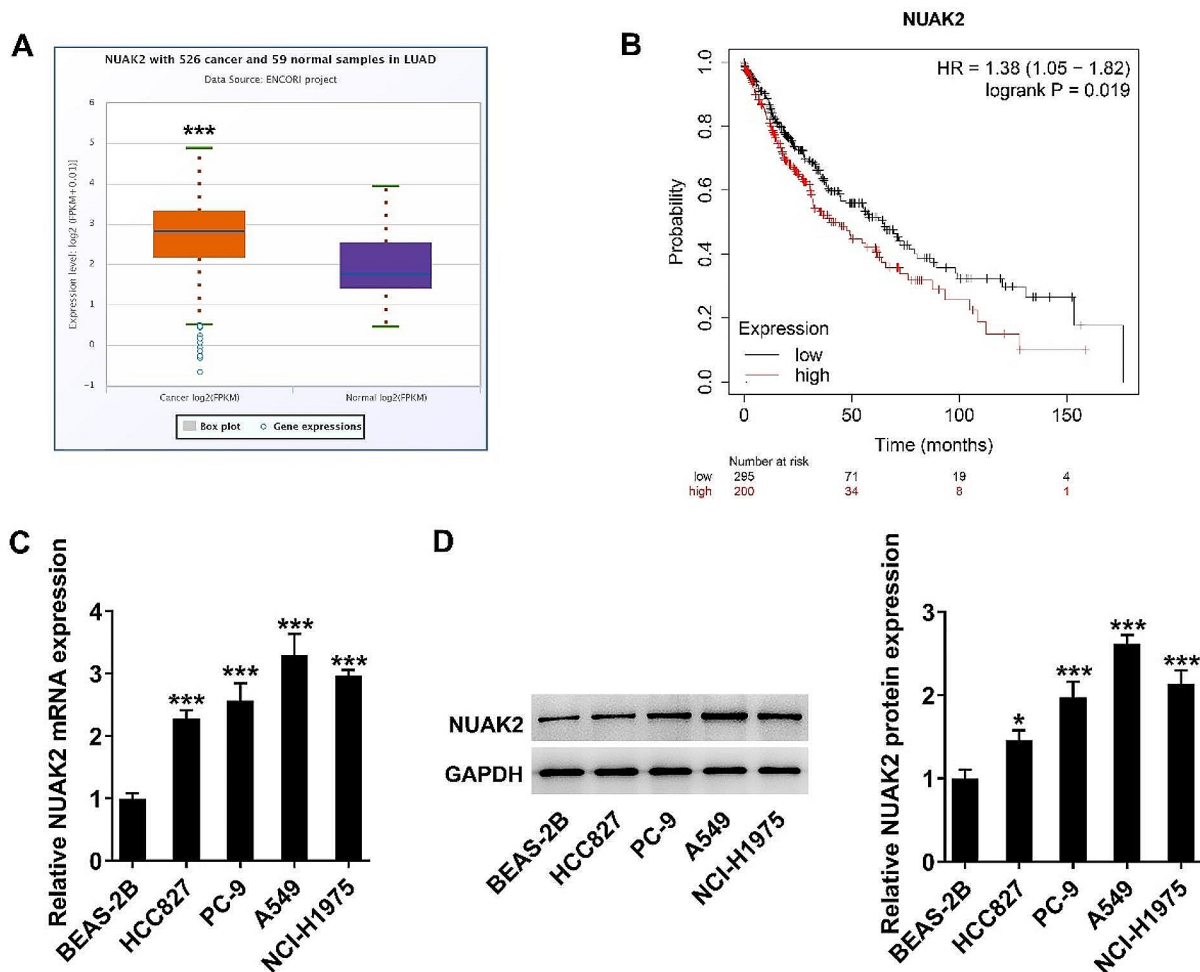


**Fig. 1** NUAK2 is upregulated in LUAD. (A) The NUAK2 expression in LUAD samples and normal samples was obtained from ENCORI database. \*\*\* $p < 0.001$ . (B) Kaplan-Meier Plotter database was used to assess NUAK2-related prognosis of patients with LUAD. (C) mRNA level and (D) protein expression of NUAK2 were detected using qRT-PCR and western blot, respectively. \* $p < 0.05$ , \*\*\* $p < 0.001$  vs. BEAS-2B

**NUAK2 depletion blocks angiogenesis and promotes senescence of A549 cells**

Next, it was observed from tube formation assay that compared to the sh-NC group, the tube structure was severely destroyed in sh-NUAK2 group (Fig. 3A). Accordingly, the expression level of VEGFR1 and VEGFR2 was significantly decreased following NUAK2 knockdown (Fig. 3B), suggesting that NUAK2 depletion restricted in vitro angiogenesis. Moreover, compared to the sh-NC group, accumulating senescence  $\beta$ -galactosidase (SA- $\beta$ -gal)-positive cells were found in the sh-NUAK2 group, accompanied with increased protein expression of p16, p21 and p53 in NUAK2-depleted A549 cells (Fig. 3C-D), revealing that NUAK2 knockdown could promote the senescence of A549 cells.

**NUAK2 depletion triggers ferroptosis in A549 cells**

Further, as NUAL2 was linked to ferroptosis, we sought to determine the effect of NUAK2 depletion on

ferroptosis in A549 cells. As exhibited from BODIPY (581/591) C11 staining, the oxidized BODIPY C11 was significantly elevated in the sh-NUAK2 group compared to the sh-NC group (Fig. 4A), confirming that NUAK2 knockdown facilitated the production of lipid ROS. Consistently, we also observed the higher thiobarbituric acid reactive substance (TBARS) production in sh-NUAK2 group than that in sh-NC group, confirming that NUAK2 knockdown increased lipid peroxidases in A549 cells (Fig. 4B). Meanwhile, NUAK2 knockdown also led to excessive  $Fe^{2+}$  level in A549 cells (Fig. 4C). Further, compared to the sh-NC group, the protein expression of SLC7A11, GPX4 and FTH1 was downregulated and the protein expression of ACSL4 was upregulated in the sh-NUAK2 group (Fig. 4D). Taken together, these findings suggested that NUAK2 knockdown enhanced ferroptosis in A549 cells.

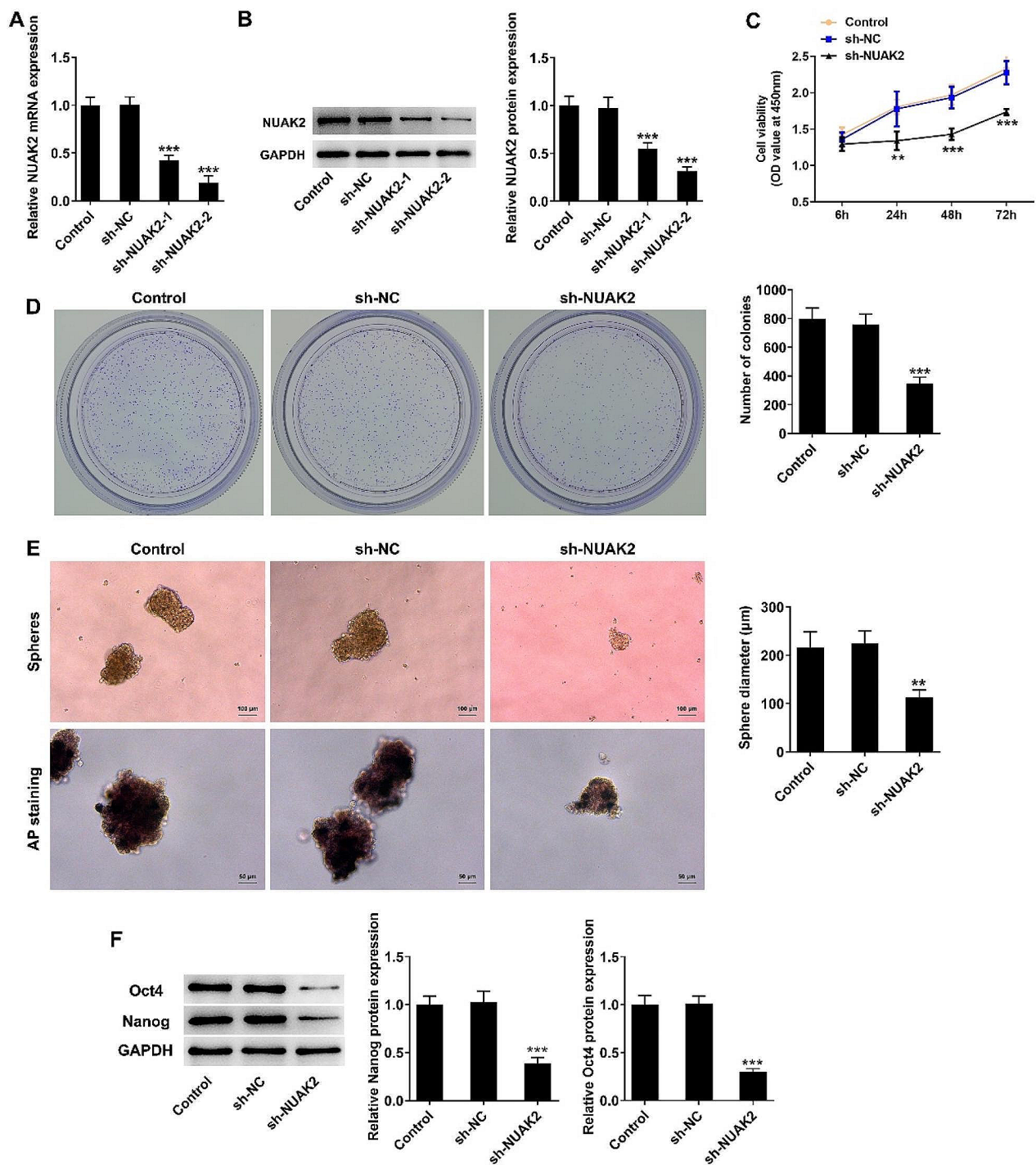


**Fig. 2** NUA2 depletion blocks the proliferation and stemness of A549 cells. **(A)** A549 cells were transfected with sh-NUAK2-1 or sh-NUAK2-2 to achieve knockdown of NUA2, and the mRNA level of NUA2 was examined by qRT-PCR. **(B)** The protein expression of NUA2 was examined by western blot. **(C)** CCK-8 assay was conducted to examine cell viability. **(D)** The colony formation assay was conducted to assess the proliferation ability. **(E)** Tumor spheres formation and AP staining assays were examined to reflect the stemness. **(F)** The protein expression of Oct4 and Nanog was examined using western blot. \*\* $p < 0.01$ , \*\*\* $p < 0.001$  vs. sh-NC

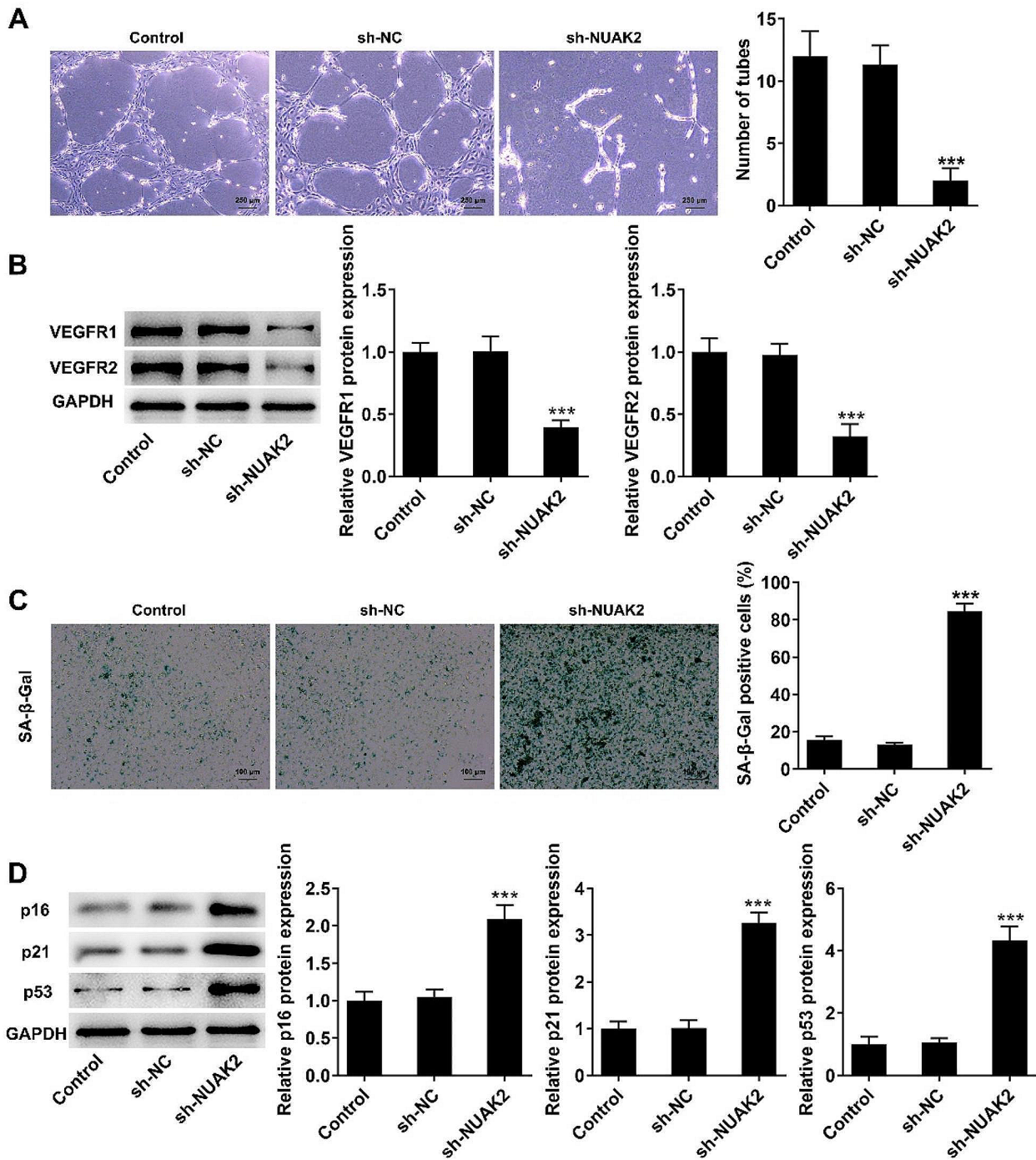


**Fig. 3** NUA2 depletion blocks angiogenesis and promotes senescence of A549 cells. **(A)** The tube formation assay was performed to assess in vitro angiogenesis. **(B)** The protein expression of VEGFR1 and VEGFR2 was examined using western blot. **(C)** SA-β-gal staining was performed to evaluate the senescence. **(D)** The protein expression of p16, p21 and p53 was examined using western blot. \*\*\* $p < 0.001$  vs. sh-NC

**Ferroptosis inhibitor partly abolishes the regulatory impacts of NUA2 depletion on cell proliferation, stemness, angiogenesis and senescence**

To clarify whether NUA2 regulated malignant behaviors of A549 cells through ferroptosis, NUA2-depleted

A549 cells were treated with ferroptosis inhibitor ferrostatin-1 (Fer-1; 1 μM) for 24 h. Compared to the sh-NUAK2 group, the cell viability and the number of colonies were significantly elevated in the Fer-1+sh-NUAK2 group (Fig. 5A-B), revealing that the Fer-1

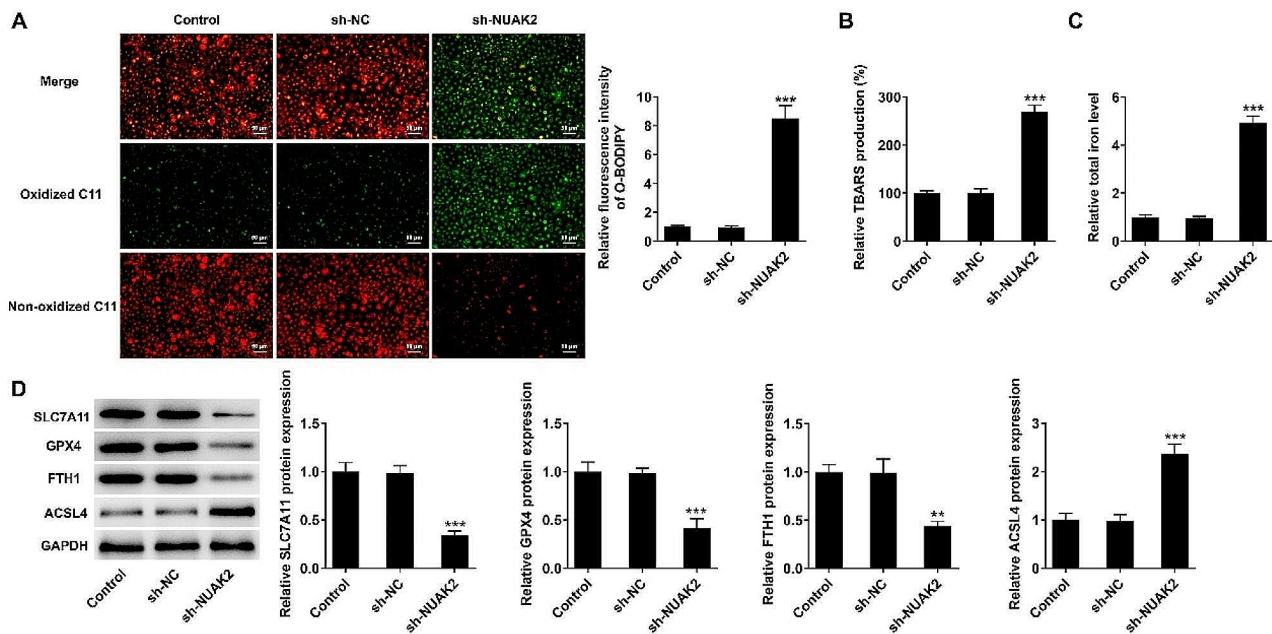


**Fig. 4** NUA2 depletion triggers ferroptosis in A549 cells. **(A)** Lipid ROS was measured by BODIPY (581/591) C11 staining. **(B)** Lipid peroxidation was determined by TBARS method. **(C)**  $\text{Fe}^{2+}$  level in A549 cells was examined using an Iron Assay kit. **(D)** Ferroptosis-related proteins were detected using western blot. \*\* $p < 0.01$ , \*\*\* $p < 0.001$  vs. sh-NC

treatment partly weakened the anti-proliferative ability of NUA2 depletion in A549 cells. Meanwhile, the inhibitory effects of NUA2 knockdown on the stemness and in vitro angiogenesis were also partially weakened by Fer-1 treatment, evidenced by the increased sphere diameter, improved tube structure, and elevated protein expressions of Oct4, Nanog, VEGFR1 and VEGFR2 in Fer-1+sh-NUAK2 group in comparison to sh-NUAK2 group (Fig. 5C-F). Further, compared to the sh-NUAK2 group, the SA- $\beta$ -gal-positive cells were remarkably declined in Fer-1+sh-NUAK2 group, and the expression levels of p16, p21 and p53 in NUA2-depleted A549 cells were significantly decreased following Fer-1 treatment (Fig. 5G-H), revealing that ferroptosis inhibition partly blocked NUA2 depletion-induced senescence in A549 cells.

#### NUAK2 depletion restricts tumor growth in mice

Finally, in vivo animal study was conducted to validate the critical role of NUA2 in LUAD. A549 cells were subcutaneously injected into the right flank of mice to establish LUAD-bearing mouse model. As observed in Fig. 6A-B, the tumor size of mice in sh-NUAK2 group was much smaller than that in the sh-NC group. Meanwhile, compared to the sh-NC group, the tumor weight was greatly decreased in the sh-NUAK2 group (Fig. 6C). Therefore, above findings demonstrated that NUA2 knockdown greatly inhibited tumor growth in LUAD-bearing mice.

#### Discussion

Lung cancer is a great threaten to human health and medical burden due to its high mobility and mortality rates [15]. Clarifying the pathogenesis of lung cancer is essential to develop effective therapeutic strategies for the treatment of lung cancer. In the present study, we identified that NUA2 was upregulated in LUAD samples and cell lines. Functionally, NUA2 depletion could significantly suppress the proliferation, stemness and angiogenesis and promote senescence of A549 cells, and also restricted tumor growth in mice. In the term of mechanism, NUA2 depletion dramatically triggered ferroptosis of A549 cells, and inhibition of ferroptosis partly weakened the anti-tumor activity of NUA2 depletion, suggesting that NUA2 depletion impeded oncogenic phenotypes of A549 cells partly via triggering ferroptosis.

Cancer stemness cells (CSCs), a special range of cancer cells, have a high capability of self-renewal, pluripotency, and tumor initiation, playing an important role in cancer metastasis, recurrence and drug resistance [16, 17]. Oct4 and Nanog are classical cancer stems cell biomarker, the high expression of which is closely associated with the recurrence and metastasis of cancers [18]. A previous study revealed that co-expression of Nanog and Oct4 induced epithelial-mesenchymal transition, enhanced CSC properties and thereby facilitated the malignancy of LUAD [19]. CircRNA circ\_POLA2 served as a potential therapeutic target for lung cancer patients due to its

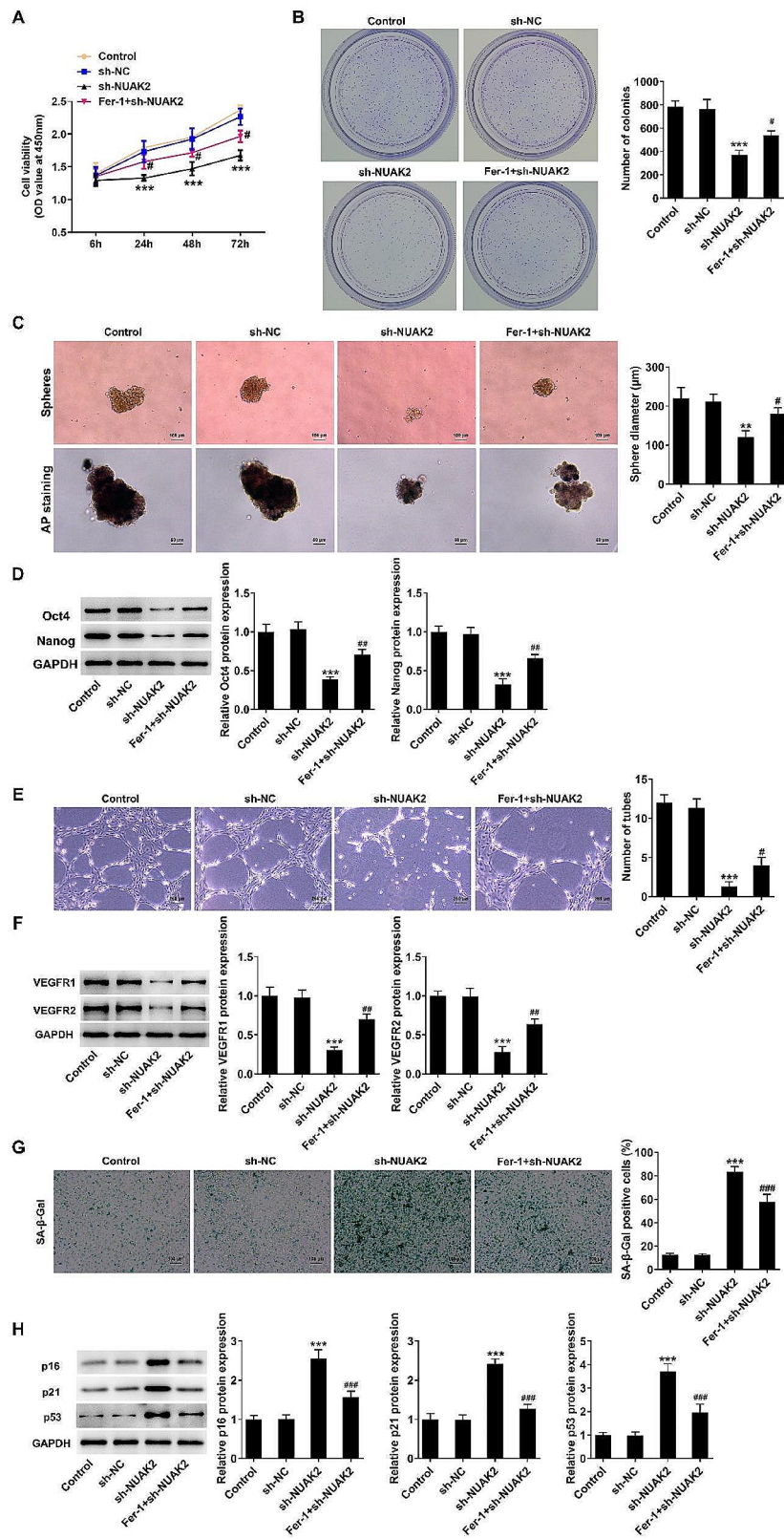


**Fig. 5** (See legend on next page.)

(See figure on previous page.)

**Fig. 5** Ferroptosis inhibitor partly abolishes the regulatory impacts of NUA2 depletion on cell proliferation, stemness, angiogenesis and senescence. **(A)** A549 cells were transfected with sh-NUAK2, with or without ferrostatin-1 (Fer-1; 1  $\mu$ M) treatment for 24 h. Cell viability was assessed using CCK-8 assay. **(B)** The colony formation assay was conducted to assess the proliferation ability. **(C)** Tumor spheres assay and AP staining assay were conducted to reflect the stemness. **(D)** The protein expression of Oct4 and Nanog was examined using western blot. **(E)** The tube formation assay was performed to assess in vitro angiogenesis. **(F)** The protein expression of VEGFR1 and VEGFR2 was examined using western blot. **(G)** SA- $\beta$ -gal staining was performed to evaluate the senescence. **(H)** The protein expression of p16, p21 and p53 was examined using western blot. \*\*\* $p < 0.001$  vs. sh-NC; # $p < 0.05$ , ## $p < 0.01$  and ### $p < 0.001$  vs. sh-NUAK2

promotive effect on lung cancer cell stemness, evidenced by enhancing sphere-formation ability and stemness marker expression (Oct4 and Nanog) [20]. Thus, we also assessed the stemness-associated transcription factors in this study. The findings exhibited that NUA2 depletion significantly declined the protein expression of Oct4 and Nanog, suggesting that the CSCs property was weakened by NUA2 depletion. In addition, the tumor spheres were also decreased following NUA2 depletion in A549 cells. Therefore, these findings demonstrated that NUA2 depletion could repress stem-like characteristics of LUAD cells.

Cellular senescence is an aging-related process characterized by an irreversible growth arrest which can prevent uncontrolled cell proliferation events [21]. Senescent cells are featured as enlarged and flat cell morphology and well-defined molecular changes, such as elevated activities of  $\beta$ -galactosidase and upregulated expressions of p16 and p21 [22, 23]. Currently, cellular senescence has been recognized as an endogenous tumor-suppressive mechanism, and considerable concern has been paid on the modulation of cellular senescence in lung cancer [24, 25]. It was reported that senescent cells within lung cancer tissues were linked to unfavorable prognosis of patients [26]. Wattanathamsan O et al. demonstrated that CAMSAP3 knockout could promote lung cancer cell senescence-associated phenotypes and restrict cell proliferation ability, thereby delaying tumor initiation and growth [27]. Zhang XL et al. identified Marchantin C as an effective natural compound preventing against lung cancer through inducing cellular senescence [28]. Therefore, developing novel regulators/drugs targeting senescence provides alternative options for cancer treatment. In terms of NUA2, a previous study demonstrated that NUA2 knockdown could induce cellular senescence and inhibit the migration of melanoma cells [29]. Consistently, in the present study, it was observed that NUA2 depletion markedly increased senescent cells (SA- $\beta$ -gal-positive), and elevated p16, p21 and p53 levels, confirming that NUA2 knockdown could facilitate cellular senescence in lung cancer cells, which might partly account for the anti-tumor activity of NUA2 depletion against lung cancer. Furthermore, the latest report evidences that senescent tumor cells have acquired vulnerability to ferroptosis induction [30]. Protein p53, a critical mediator of senescence, can also modulate the response to ferroptosis via GPX4-dependent

and GPX4-independent pathway [31]. Consistently, it was revealed in this study that NUA2 knockdown facilitated cellular senescence in A549 cells, accompanied with upregulated p53/GPX4 and enhanced ferroptosis. However, the complex connection between senescence and ferroptosis is little research to date [32]. Although we further demonstrated that ferroptosis inhibition could weaken NUA2 knockdown-induced senescence in A549 cells, the detailed mechanisms are required to be investigated.

Some limitations are presented in this study. On the one hand, more shRNAs in cell phenotype assays are required to exclude the shRNA off-target possibility. On the other hand, this study raised multiple aspects (such as senescence, stemness and angiogenesis) through which NUA2 contributed to the progression of LUAD, while detailed mechanism on the association among NUA2, NUA2-mediated ferroptosis and these aspects are required to be explored in our future work.

## Conclusion

In summary, this work, for the first time, disclosed that NUA2 was upregulated in lung cancer and contributed to the tumorigenesis and metastasis of lung cancer. NUA2 depletion hindered the in vitro malignant behaviors of A549 cells and restricted in vivo tumor growth partially through triggering ferroptosis. NUA2 might be an effective therapeutic approach for the targeted therapy of clinical treatment of lung cancer.

## Methods and materials

### Bioinformatic analysis

The gene expression of NUA2 in LUAD samples ( $n=526$ ) and the normal samples ( $n=59$ ) was obtained from the Encyclopedia of RNA Interactomes portal (ENCORI, <https://rna.sysu.edu.cn/encori/index.php>) [33]. Kaplan-Meier Plotter (<https://kmplot.com/analysis/>) database [34] was utilized to predict the prognosis of NUA2 in LUAD.

### Cell culture

Human normal lung epithelial cells (BEAS-2B) were obtained from iCell (Shanghai, China) and were incubated with Dulbecco's Modified Eagle Medium (DMEM; Gibco, Thermo Fisher Scientific, Inc., Waltham, MA, USA) supplemented with 10% fetal bovine serum (FBS; Gibco) and 1% penicillin/streptomycin (P/S). Human

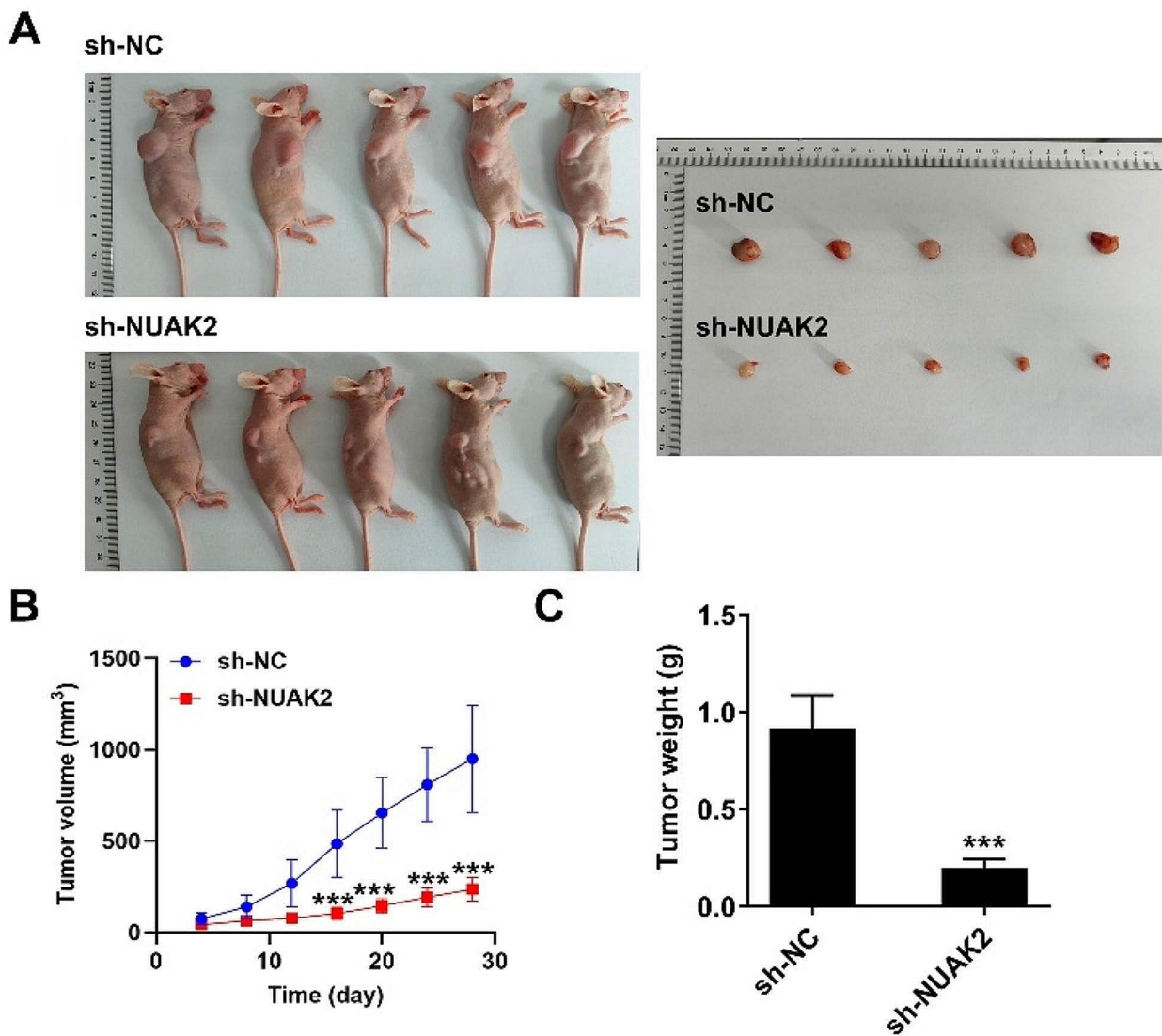


**Fig. 6** NUA2 depletion restricts tumor growth in mice. **(A)**  $4 \times 10^6$  A549 cells with sh-NC or sh-NUAK2 were subcutaneously injected into the right flank of mice. After sacrifice, tumors were observed. **(B)** Tumor volume was measured each four days. **(C)** After sacrifice, the tumor weight was recorded. \*\*\* $p < 0.001$  vs. sh-NC

lung cancer cell lines (HCC827, PC-9, A549 and NCI-H1975) were obtained from Procell (Wuhan, China), and A549 cells were incubated with F12K Medium (Gibco) while the other cells were incubated with Roswell Park Memorial Institute (RPMI)-1640 medium, supplemented with 10% FBS and 1% P/S. All cells were maintained at 37 °C in a humidified incubator with 5% CO<sub>2</sub>.

#### Total RNA isolation and quantitative real-time PCR (qRT-PCR)

Total RNA was isolated from A549 cells using TRIzol reagent (Invitrogen; Thermo Fisher Scientific, Inc.) in line with the guidelines. Subsequently, 1  $\mu\text{g}$  of total RNA was reverse transcribed into cDNA using the Prime-Script

one-step RT-PCR kit (Takara, Dalian, China). Thereafter, qRT-PCR was carried out using iQTM SYBR Supermix (Bio-Rad, Hercules, CA, USA) on an ABI PRISM 7300 detection system (Applied Biosystems; Thermo Fisher Scientific, Inc.). The relative mRNA level of genes was calculated using the  $2^{-\Delta\Delta C_q}$  method and normalized to the internal standard GAPDH.

#### Western blot

A549 cells were lysed using RIPA lysis buffer. After centrifugation, the supernatant was harvested and the total protein concentration was detected utilizing the BCA protein assay kit (Beyotime, Shanghai, China). Subsequently, SDS-polyacrylamide gel electrophoresis

(SDS-PAGE; Beyotime) was used to separate proteins, and the segregated proteins were transferred onto polyvinylidene fluoride (PVDF) membranes (Merck Millipore, Germany). After being blocked with nonfat milk, the membranes were probed with primary antibodies at 4 °C overnight, and then incubated with secondary antibodies at room temperature for 2 h. Eventually, the protein bands were developed using an enhanced chemiluminescence kit (ECL; Beyotime).

#### Cell transfection

Short hairpin RNAs targeting NUA2 (sh-NUAK2-1 and sh-NUAK2-2) were obtained from GenePharma (Shanghai, China), and the empty plasmid acted as the negative control (sh-NC). When achieved 60–70% confluence, A549 cells were transfected with sh-NC or sh-NUAK2-1/sh-NUAK2-2 using Lipofectamine 3000 reagent (Invitrogen) strictly in line with the manufacturer's protocol. 48 h post transfection, the transfected cells were harvested for following experiments.

#### Cell viability

Cell viability was assessed using Cell Counting Kit (CCK-8; Yeasen, China) following the manufacturer's instructions. In brief, A549 cells were inoculated into 96-well plates at a density of  $1 \times 10^3$  cells/well. After incubation at 37 °C for 6 h, 24 h, 48 h and 72 h, respectively, the CCK-8 reagent was added to each well, and the plates were incubated at 37 °C for 3 h. Eventually, the plates were measured by a microplate reader (Bio-Tek Instruments, Wibooski, VT, USA) to obtain the absorbance at 450 nm.

#### Colony formation assay

Cells were inoculated into 6-well plates and cultured at 37 °C in a humidified incubator with 5% CO<sub>2</sub>. After 2 weeks, cells were fixed with 100% methanol and stained with 0.1% crystal violet at room temperature. The visible colonies with more than 50 cells were photographed.

#### Spheroid formation assay and AP staining

A549 cells were cultured with F12K Medium containing 5 mg/L of heparin, 20 µg/L of hEGF, 2% B27, and 10 µg/L of bFGF in Ultra-Low Attachment 6-well plate (Costar, Corning, NY, USA). After incubation for 10 days, the tumor spheres (sphere diameter over 50 µm) were photographed. In addition, for the assessment of pluripotent stem cells, Alkaline Phosphatase Stain Kit (Yeasten) was applied. In brief, after the growth medium was removed, the spheroids were stained with AP staining reagent for 30 min for visualization in line with the protocols of the product.

#### Tube formation assay

In vitro tube formation assay was conducted to assess angiogenesis ability. In brief, transfected A549 cells were inoculated into 6-well plates for 24 h. The culture medium was then changed to serum-free medium and cells were incubated at 37 °C for another 48 h. The supernatant was collected as the conditional medium.  $2 \times 10^4$  HUVECs were inoculated into 96-well plates which were pre-coated with Matrigel (BD Biosciences, Billerica, MA, USA) and were cultured with above conditional medium from each group. After incubation at 37 °C for 12 h, the tube structures were photographed by microscopy.

#### Senescence-Associated β-Galactosidase staining

A549 cells were fixed with 4% paraformaldehyde for 15 min. After washing, cells were stained with SA-β-gal (Beyotime) at 37 °C in the darkness overnight in line with the manufacturer's guidelines. The SA-β-gal-positive cells were photographed by a light microscopy (Olympus, Tokyo, Japan).

#### Thiobarbituric acid reactive substance (TBARS) assay

Lipid peroxidation was assessed by TBARS assay. In brief, A549 cells were incubated with trichloroacetic acid and butylated hydroxyanisole. After centrifugation, the collected supernatant was mixed with trichloroacetic acid again, followed by boiling. Eventually, a microplate reader (Bio-Tek Instruments) was used to obtain the absorbance at 450 nm.

#### BODIPY (581/591) C11 staining

Lipid ROS was measured by BODIPY (581/591) C11 staining (Invitrogen) according to the manufacturer's protocols. In brief, cells were inoculated into 6-well plates and cultured at 37 °C in a humidified incubator with 5% CO<sub>2</sub>. After washed with PBS, cells were incubated with 10 µM BODIPY (581/591) C11 at 37 °C in the darkness for 30 min. Eventually, fluorescence was measured using an inverted fluorescence microscope (Olympus).

#### Assessment of iron level

An Iron Assay kit (Abcam, Cambridge, UK) was used to assess levels of Fe<sup>2+</sup> in A549 cells. In brief, the cell lysates were incubated with iron probe at 37 °C for 60 min away from the light in line with the manufacturer's instructions. The microplate reader (Bio-Tek Instruments) was used to obtain the absorbance at 593 nm.

#### Animal study

10 male BALB/c-nu mice (4–6-week-old; 18–20 g) obtained from Shanghai SLAC Laboratory Animal Center were kept in a standard environment with free access to water and food. All animal studies were carried in compliance with the ARRIVE guidelines and

were approved by the First Affiliated Hospital of Nanjing Medical University.  $4 \times 10^6$  A549 cells with sh-NC or sh-NUAK2 were subcutaneously injected into the right flank of mice. The tumor volume was monitored every four days with the formula: Tumor volume = Length  $\times$  width<sup>2</sup>/2. Mice were sacrificed on the day 28 following cell injection, and tumors were harvested for weighing.

### Statistical analysis

All data are presented as mean  $\pm$  standard deviation (SD). All statistical analyses were carried out using GraphPad Prism (GraphPad Software, San Diego, CA, USA). The differences among groups were analyzed by analysis of variance (ANOVA), followed by Tukey's post hoc test.  $P < 0.05$  was considered to indicate statistically significant.

### Supplementary Information

The online version contains supplementary material available at <https://doi.org/10.1186/s13008-024-00128-8>.

Supplementary Material 1

### Acknowledgements

Not applicable.

### Author contributions

JL designed the study; JF, LX and HL conducted the experiments and analyzed the data; JF drafted the manuscript and JL critically revised the manuscript. All authors confirmed the final version of the manuscript.

### Funding

This study was supported by the WU JIEPING MEDICAL FOUNDATION (grant No. 320.6750.19008).

### Data availability

No datasets were generated or analysed during the current study.

### Declarations

### Ethical approval

All animal studies were approved by the First Affiliated Hospital of Nanjing Medical University.

### Conflict of interest

The authors have declared that no conflict of interest exists.

### Author details

<sup>1</sup>Department of Thoracic Surgery, the First Affiliated Hospital of Nanjing Medical University, No. 300 Guangzhou Road, Gulou District, Nanjing 210000, Jiangsu, China

Received: 15 March 2024 / Accepted: 22 July 2024

Published online: 28 July 2024

### References

- Siegel RL, Miller KD, Wagle NS, Jemal A. Cancer statistics, 2023. *CA Cancer J Clin.* 2023;73(1):17–48. <https://doi.org/10.3322/caac.21763>.
- Xu JY, Zhang C, Wang X, Zhai L, Ma Y, Mao Y et al. Integrative Proteomic Characterization of Human Lung Adenocarcinoma. *Cell.* 2020;182(1):245–61 e17. <https://doi.org/10.1016/j.cell.2020.05.043>.
- Siegel RL, Miller KD, Jemal A. Cancer statistics, 2019. *CA Cancer J Clin.* 2019;69(1):7–34. <https://doi.org/10.3322/caac.21551>.
- Lei G, Zhuang L, Gan B. Targeting ferroptosis as a vulnerability in cancer. *Nat Rev Cancer.* 2022;22(7):381–96. <https://doi.org/10.1038/s41568-022-00459-0>.
- Dixon SJ, Lemberg KM, Lamprecht MR, Skouta R, Zaitsev EM, Gleason CE, et al. Ferroptosis: an iron-dependent form of nonapoptotic cell death. *Cell.* 2012;149(5):1060–72. <https://doi.org/10.1016/j.cell.2012.03.042>.
- Liu Y, Fan X, Zhao Z, Shan X. LncRNA SLC7A11-AS1 contributes to Lung Cancer Progression through facilitating TRAIIP expression by inhibiting miR-4775. *Onco Targets Ther.* 2020;13:6295–302. <https://doi.org/10.2147/OTT.S253082>.
- Huang F, Pang J, Xu L, Niu W, Zhang Y, Li S, et al. Hedyotis diffusa injection induces ferroptosis via the Bax/Bcl2/VDAC2/3 axis in lung adenocarcinoma. *Phytomedicine.* 2022;104:154319. <https://doi.org/10.1016/j.phymed.2022.154319>.
- Bonnard C, Navaratnam N, Ghosh K, Chan PW, Tan TT, Pomp O, et al. A loss-of-function NUA2 mutation in humans causes anencephaly due to impaired Hippo-YAP signaling. *J Exp Med.* 2020;217(12). <https://doi.org/10.1084/jem.20191561>.
- Namiki T, Coelho SG, Hearing VJ. NUA2: an emerging acral melanoma oncogene. *Oncotarget.* 2011;2(9):695–704. <https://doi.org/10.18632/oncotarget.325>.
- Tang L, Tong SJ, Zhan Z, Wang Q, Tian Y, Chen F. Expression of NUA2 in gastric cancer tissue and its effects on the proliferation of gastric cancer cells. *Exp Ther Med.* 2017;13(2):676–80. <https://doi.org/10.3892/etm.2016.3983>.
- Guo Z, Guo L. OTUD7B deubiquitinates and stabilizes YAP1 to upregulate NUA2 expression, thus accelerating gastric cancer progression. *Dig Liver Dis.* 2024;56(2):352–62. <https://doi.org/10.1016/j.dld.2023.06.026>.
- Chen B, Wang B, Xu X, Chen X, Yi W, Xu S, et al. Upregulation of NUA2: a novel prognostic marker in breast cancer. *Histol Histopathol.* 2023;38(7):811–22. <https://doi.org/10.14670/HH-18-554>.
- Dai Y, Shi W, Qiu Y, Xu T, Lin J, Su Y. Circ\_0000033 up-regulates NUA2 by sequestering miR-378a-3p to promote breast tumorigenesis. *Environ Mol Mutagen.* 2023;64(6):359–70. <https://doi.org/10.1002/em.22558>.
- Singh T, Beatty A, Peterson JR. The AMPK-related kinase NUA2 suppresses glutathione peroxidase 4 expression and promotes ferroptotic cell death in breast cancer cells. *Cell Death Discov.* 2022;8(1):253. <https://doi.org/10.1038/s41420-022-01044-y>.
- Zeng J, Li X, Liang L, Duan H, Xie S, Wang C. Phosphorylation of CAP1 regulates lung cancer proliferation, migration, and invasion. *J Cancer Res Clin Oncol.* 2022;148(1):137–53. <https://doi.org/10.1007/s00432-021-03819-9>.
- Zhou G, Latchoumanan O, Bagdesar M, Hebbard L, Duan W, Liddle C, et al. Aptamer-based therapeutic approaches to Target Cancer Stem cells. *Theranostics.* 2017;7(16):3948–61. <https://doi.org/10.7150/thno.20725>.
- Clevers H. The cancer stem cell: premises, promises and challenges. *Nat Med.* 2011;17(3):313–9. <https://doi.org/10.1038/nm.2304>.
- Battle E, Clevers H. Cancer stem cells revisited. *Nat Med.* 2017;23(10):1124–34. <https://doi.org/10.1038/nm.4409>.
- Chiou SH, Wang ML, Chou YT, Chen CJ, Hong CF, Hsieh WJ, et al. Coexpression of Oct4 and nanog enhances malignancy in lung adenocarcinoma by inducing cancer stem cell-like properties and epithelial-mesenchymal transdifferentiation. *Cancer Res.* 2010;70(24):10433–44. <https://doi.org/10.1158/0008-5472.CAN-10-2638>.
- Fan Z, Bai Y, Zhang Q, Qian P. CircRNA circ\_POLA2 promotes lung cancer cell stemness via regulating the miR-326/GNB1 axis. *Environ Toxicol.* 2020;35(10):1146–56. <https://doi.org/10.1002/tox.22980>.
- Campisi J. Aging, cellular senescence, and cancer. *Annu Rev Physiol.* 2013;75:685–705. <https://doi.org/10.1146/annurev-physiol-030212-183653>.
- Hernandez-Segura A, Nehme J, Demaria M. Hallmarks of Cellular Senescence. *Trends Cell Biol.* 2018;28(6):436–53. <https://doi.org/10.1016/j.tcb.2018.02.001>.
- Volonte D, Sedorovitz M, Galbiati F. Impaired Cdc20 signaling promotes senescence in normal cells and apoptosis in non-small cell lung cancer cells. *J Biol Chem.* 2022;298(10):102405. <https://doi.org/10.1016/j.jbc.2022.102405>.
- Alexa-Stratulat T, Pavel-Tanasa M, Cianga VA, Antoniu S. Immune senescence in non-small cell lung cancer management: therapeutic relevance, biomarkers, and mitigating approaches. *Expert Rev Anticancer Ther.* 2022;22(11):1197–210. <https://doi.org/10.1080/14737140.2022.2139242>.
- Zhu H, Sun J, Zhang C, Li P, Tan C, Yang M, et al. Cellular Senescence in Non-small Cell Lung Cancer. *Front Biosci (Landmark Ed).* 2023;28(12):357. <https://doi.org/10.31083/j.fbl2812357>.
- Ferrara R, Naigeon M, Auclin E, Duchemann B, Cassard L, Jouniaux JM, et al. Circulating T-cell immunosenescence in patients with Advanced Non-small Cell Lung Cancer treated with single-agent PD-1/PD-L1 inhibitors or

- platinum-based Chemotherapy. *Clin cancer Research: Official J Am Association Cancer Res.* 2021;27(2):492–503. <https://doi.org/10.1158/1078-0432.CCR-20-1420>.
27. Wattanathamsan O, Chetprayoon P, Chantaravisoot N, Wongkongkathep P, Chanvorachote P, Pongrakhananon V. CAMSAP3 depletion induces lung cancer cell senescence-associated phenotypes through extracellular signal-regulated kinase inactivation. *Cancer Med.* 2021;10(24):8961–75. <https://doi.org/10.1002/cam4.4380>.
  28. Zhang XL, Ji XT, Sun B, Qian LL, Hu XL, Lou HX, et al. Anti-cancer effect of marchantin C via inducing lung cancer cellular senescence associated with less secretory phenotype. *Biochim Biophys Acta Gen Subj.* 2019;1863(10):1443–57. <https://doi.org/10.1016/j.bbagen.2019.05.006>.
  29. Namiki T, Tanemura A, Valencia JC, Coelho SG, Passeron T, Kawaguchi M, et al. AMP kinase-related kinase NUAK2 affects tumor growth, migration, and clinical outcome of human melanoma. *Proc Natl Acad Sci U S A.* 2011;108(16):6597–602. <https://doi.org/10.1073/pnas.1007694108>.
  30. Zhu X, Fu Z, Dutchak K, Arabzadeh A, Milette S, Steinberger J, et al. Cotargeting CDK4/6 and BRD4 promotes senescence and ferroptosis sensitivity in Cancer. *Cancer Res.* 2024;84(8):1333–51. <https://doi.org/10.1158/0008-5472.Can-23-1749>.
  31. Liu Y, Gu W. p53 in ferroptosis regulation: the new weapon for the old guardian. *Cell Death Differ.* 2022;29(5):895–910. <https://doi.org/10.1038/s41418-022-00943-y>.
  32. Coradduzza D, Congiargiu A, Chen Z, Zinellu A, Carru C, Medici S. Ferroptosis and senescence: a systematic review. *Int J Mol Sci.* 2023;24(4). <https://doi.org/10.3390/ijms24043658>.
  33. Li JH, Liu S, Zhou H, Qu LH, Yang JH. *Nucleic Acids Res.* 2014;42(Database issue):D92–7. <https://doi.org/10.1093/nar/gkt1248>. starBase v2.0: decoding miRNA-ceRNA, miRNA-ncRNA and protein-RNA interaction networks from large-scale CLIP-Seq data.
  34. Gyorffy B. Transcriptome-level discovery of survival-associated biomarkers and therapy targets in non-small-cell lung cancer. *Br J Pharmacol.* 2024;181(3):362–74. <https://doi.org/10.1111/bph.16257>.

### Publisher's Note

Springer Nature remains neutral with regard to jurisdictional claims in published maps and institutional affiliations.